The variations of VOCs based on the policy change of Omicron in traffic-hub city Zhengzhou

Bowen Zhang[1, 3], Dong Zhang[2, 3], Zhe Dong[2, 3], Xinshuai Song[1, 3], Ruiqin Zhang[1, 3], Xiao Li[1, 3,*]

[1]School of Ecology and Environment, Zhengzhou University, Zhengzhou 450001, China

[2]College of Chemistry, Zhengzhou University, Zhengzhou 450001, China

[3]Institute of Environmental Sciences, Zhengzhou University, Zhengzhou 450001, China

Correspondence to: Xiao Li, E-mail address: lixiao9060@zzu.edu.cn

Abstract: Online volatile organic compounds (VOCs) were monitored before and after the Omicron policy change at an urban site in polluted Zhengzhou from December 1, 2022, to January 31, 2023. The characteristics and sources of VOCs were investigated. The daily mean concentrations of $PM_{2.5}$ and total VOCs (TVOCs) ranged from 53.5 to 239.4 µg/m³ and 15.6 to 57.1 ppbv, respectively, with mean values of 111.5 ± 45.1 µg/m³ and 36.1 ± 21.0 ppbv, respectively, throughout the period. Two severe pollution events (designated as Case 1 and Case 2) were identified in accordance with the National Ambient Air Quality Standards (NAAQS) (China's National Ambient Air Quality Standards (NAAQS) from 2012). Case 1 (December 5 to December 10, $PM_{2.5}$ daily mean = 142.5 µg/m³) and Case 2 (January 1 to January 8, $PM_{2.5}$ daily mean = 181.5 µg/m³) occurred during the infection period (when the policy of "full nucleic acid screening measures" was in effect) and the recovery period (after the policy was cancelled), respectively. The $PM_{2.5}$ and TVOCs values for Case 2 are, respectively, 1.3 and 1.8 times higher than those for Case 1. The precise influence of disparate meteorological circumstances on the two pollution incidents is not addressed in this study. The results of the positive matrix factor modeling demonstrated that the primary source of volatile organic compounds (VOCs) during the observation period was industrial emissions, which constituted 32% of the total VOCs, followed by vehicle emissions (27%) and combustion (21%). In Case 1, industrial emissions constituted the primary source of VOCs, accounting for 32% of the total VOCs. In contrast, in Case 2, the contribution of vehicular emission sources increased to 33% and became the primary source of VOCs. The secondary organic aerosol formation potential for Case 1 and Case 2 were found to be 37.6 µg/m³ and 65.6 µg/m³, respectively. In Case 1, the

34   largest contribution of SOAP from industrial sources accounted for the majority (63%,

35   23.8 μg/m³), followed by vehicular sources (18%). After the end of the epidemic and

36   the resumption of productive activities in the society, the difference in the proportion

37   of SOA generated from various sources decreased. Most of the SOAP came from

38   solvent use and fuel evaporation sources, accounting for 32% (20.9 μg/m³) and 26%

39   (16.8 μg/m³), respectively. On days with minimal pollution, industrial sources and

40   solvent use remain the main contributors to SOA formation. Therefore, regulation of

41   emissions from industry, solvent-using industries and motor vehicles need to be

42   prioritized to control the PM$_{2.5}$ pollution problem.

43

1. Introduction

Volatile organic compounds (VOCs) in the atmosphere have high reactivity and can react with nitrogen oxides (NO_x) to form a series of secondary pollutants such as ozone (O_3) and secondary organic aerosol (SOA), resulting in regional air pollution (Li et al., 2019; Hui et al., 2020). The problem of O_3 pollution has been plaguing major urban agglomerations in China (Zheng et al., 2010; Li et al., 2014; Wang et al., 2017). SOA is an important component of fine particulate matter ($PM_{2.5}$) and contributes significantly to haze pollution (Liu et al., 2019). $PM_{2.5}$ remains the most significant air pollutant in many Chinese cities for years (Shao et al., 2016; Wu et al., 2016). In addition, VOCs, represented by the benzene homologues, can cause damage to kidneys, liver, and nervous system of humans when they enter the body (Zhang et al., 2018).

Studies have shown that the most common VOC components in China are alkanes, olefins, aromatic hydrocarbons, oxygenated VOCs (OVOCs), and halogenated hydrocarbons, among which alkanes are the most abundant species (Liu et al., 2020; Zhang et al., 2021a). VOCs in the atmosphere have a wide range of sources, and VOCs in different regions are affected by multiple factors such as local geography, climate, and human activities (Mu et al., 2023; Zou et al., 2023). The above reasons lead to significant regional and seasonal differences in the characteristics of VOCs (Song et al., 2021). For example, the annual average concentration of VOCs in the coastal background area of the Pearl River Delta is 9.3 ppbv. The seasonal variation trend of VOCs is high in autumn and winter and low in summer (Yun et al., 2021). In contrast, the average VOC concentration in autumn and winter in Beijing was 22.6 ± 12.6 ppbv, and the VOC concentration in the winter heating period was twice that in the autumn non-heating period (Niu et al., 2022).

Moreover, the sources of VOC components in different regions are also related to the local industrial structure and living habits. In rural areas of North China Plain in winter, it is found that the SOA formation potential (SOAP) of VOCs under low NO_x conditions is significantly higher than that under high NO_x conditions, and the increase of aromatic hydrocarbon emissions caused by coal combustion is the main reason for the higher SOAP in winter (Zhang et al., 2020). Li et al. (2022) found that the average increased concentration of acetylene was 4.8 times from autumn to winter in the Guanzhong Plain, indicating that fuel combustion during the heating period in winter has a significant impact on the composition of VOCs. In contrast, continuous

observations conducted by Zhou et al. (2022) in the suburbs of Dongguan in summer found that industrial solvent usage, liquefied petroleum gas (LPG) and oil and gas volatilization were the main sources of VOCs. The results highlighted a wide variation of characteristics, sources and chemical reactions of VOCs in the atmosphere thus it is necessary to investigate VOCs in different cities when formulating control measures.

Zhengzhou, as the capital of Henan Province, is an important transportation hub and economic center in the Central Plains region. Zhengzhou is currently facing significant air pollution problems, with the Air Quality Index at the bottom of the national ranking of 168 cities for many years. In January 2023, for example, the number of polluted days with $PM_{2.5}$ as the primary pollutant was 17, and the daily average value of $PM_{2.5}$ reached a maximum of 298 $\mu g/m^3$ (https://www.aqistudy.cn/historydata/daydata.php?city=%E9%83%91%E5%B7%9E &month=202301, Accessed Jan 2024), which is almost 300% higher than the Chinese daily average standard (grade II, 75 $\mu g/m^3$). The studies of VOCs were carried out in Zhengzhou in recent years, which focused on the characteristics and sources of VOCs during pollution episodes (Lai et al., 2024) or before the coronavirus epidemic outbreak (Li et al., 2020; Zhang et al., 2021b). While some atmospheric VOCs studies involving the impact of Covid-19 lockdown have been performed in India (Singh et al., 2023a), in China (e.g., Pei et al., 2022; Jensen et al., 2023; Zuo et al., 2024), or with respect to toluene, benzene, m/p-xylene and ethylbenzene only (e.g., Sahu et al., 2022; Singh et al., 2023b), a gap persisted in the investigation of VOCs due to the impact of abolishment of China's zero-policy. Furthermore, some studies have discussed the impact of changes in human production activities on air pollution during and after the outbreak of the coronavirus disease (e.g., Ma et al., 2022; Jiang et al., 2023; Song et al., 2023), but as mentioned earlier, only a few studies with in-depth exploration of the changes in VOCs and none dealing with ending the zero-Covid policy during Omicron variant infection period.

In this study, we conducted continuous online observations of VOCs during the polluted winter season at an urban site in Zhengzhou. The study covered the period following the removal of lockdown measures. We focused on pollution events when the daily average $PM_{2.5}$ concentration exceeded 75 $\mu g/m^3$ (China's Class II standard) for more than three consecutive days. Days with $PM_{2.5}$ concentrations below 35 $\mu g/m^3$ (China's Class I standard) were classified as clean days. During this period, China lifted zero-COVID strategies, announcing the '10 measures' for optimizing COVID-19 rules

113   on December 7, 2022 (http://www.news.cn/politics/2022-12/07/c_1129189285.htm,

114   Accessed Jan 2024). Zhengzhou's epidemic prevention and control measures changed

115   with the issuance of Circular No. 163 on December 4, 2022, which allowed the

116   reopening of closed public places. As a result, movement within Zhengzhou increased

117   and social production resumed. Our research specifically examines the period

118   dominated by the COVID-19 Omicron variant. where they demonstrate notable

119   differences from the early virus strains (i.e., original SARS-CoV-2 virus and Delta) in

120   terms of geographical transmission, the scale of the infected population, and symptom

121   manifestation (Petersen et al., 2022; Merino et al., 2023).

122   After the quarantine policy was lifted, people basically rested at home due to

123   infection or fear of infection with Omicron. The resumption of normal production and

124   life depends on herd immunization. This outbreak event is the longest in duration and

125   the largest in number of infections since the 2020 outbreak of the novel coronavirus in

126   Zhengzhou. It would be beneficial to investigate the impact of this event on emissions

127   related to transportation and industrial production. This change is worth exploring in

128   terms of its impact on transportation and industrial production emissions. Therefore,

129   the characteristics and variations of VOCs during different periods were investigated to

130   assess their impact on the formation of SOA and to provide data support for future

131   pollution control policies in Zhengzhou.

132

2. Materials and methods

2.1 Sample collection and Chemical analysis

The online VOCs observation station is located on the roof of the Zhengzhou Environmental Protection Monitoring Center, which is in the urban area. The sampling site is close to main roads on three sides (150 m away from Funiu Road on the east side, 200 m away from Qinling Road on the west side, and connected to Zhongyuan Road on the south side), and surrounded by residential areas and commercial areas without other large nearby stationary sources. The sampling period for this study was from December 1, 2022, to January 31, 2023, and serious $PM_{2.5}$ pollution in Zhengzhou was of frequent occurrence during December and January. (https://www.aqistudy.cn/historydata/monthdata.php?city=%e9%83%91%e5%b7%9e #:~:text=%E7%94%9F%E5%91%BD%E6%9D%A5%E6%BA%90%E8%87%AA% E7%84%B6%EF%BC%8C%E5%81%A5). Apart from a brief occurrence of rain and snow on December 25, the sampling days were either sunny or cloudy. The wind speed (WS), temperature (Temp) and relative humidity (RH) during this period were 1.3 ± 0.9 m/s, 5.3 ± 3.2 ℃ and $38.9 \pm 19.0\%$), respectively, similar to the values observed in previous years in Zhengzhou. It is interesting to point out that the sampling period in the present study covered the entire infection period of Omicron in Zhengzhou, including the phase of surge in infected population (Infection period, from 2022.12.01 to 2022.12.31) and restoration of production and livelihood phase (Recovery period, from 2023.1.1 to 2023.1.31 in 2023) (Fig. S1, Chinese Center for Disease Control and Prevention, 2023).

The VOCs were measured hourly using a GC-FID/MS (TH-PKU 300 b, Wuhan Tianhong Instruments Co., China). The instrument TH-PKU300b includes electronic refrigeration ultra-low temperature pre-concentration sampling system, analysis system and system control software. The ambient VOCs in the first 5 minutes of each hour were collected by the sampling system and then entered the concentration system. Under low temperature conditions, the VOCs samples collected were frozen in the capillary capture column, and then quickly heated and resolved, so that the compounds entered the analysis system. After separation by chromatographic column, the compounds were monitored by FID and MS detectors. During the detection process, the atmospheric samples collected undergo analysis through two distinct pathways. C2-C5 hydrocarbons are analyzed using FID, while C5-C12 hydrocarbons, halocarbons,

and OVOCs are analyzed with a MS detector. After excluding species with missing data exceeding 10%, the detected volatile organic compounds include 29 alkanes, 11 alkenes, 17 aromatics, 35 halocarbons, 12 OVOCs, 1 alkyne (acetylene), and 1 sulfide (CS_2) with a total of 106 compounds. A detailed description of the instrumentation can be found in our previous study (Zhang et al., 2021b; Shi et al., 2022; Zhang et al., 2024).

The instrument was calibrated per week to ensure the accuracy of VOCs by injecting standard gases with a five-point calibration curve. The detection limit of C2-C5 hydrocarbons ranges from 0.007 to 0.099 ppbv, other hydrocarbons are 0.004–0.045 ppbv, halogenated hydrocarbons 0.009-0.099 ppbv, OVOCs and other compounds of 0.006–0.095 ppbv. Thirty-two of the monitored VOCs had over 90% observed data greater than the detection limit, and 34 had more than 50% observed data greater than the detection limit.

Simultaneous observations at the same site were also carried out for particulate matter ($PM_{2.5}$, PM_{10}), other trace gases (carbon monoxide (CO), O_3, nitric oxide (NO), nitrogen dioxide (NO_2)), and meteorological data (Temperature, RH, WS, and wind direction (WD)) based on 1 h resolution.

2.2 Positive Matrix Factorization (PMF) model

EPA PMF5.0 model was used for the quantitative source analysis of VOCs (Norris et al., 2014). The principles and methods have been described in detail in previous studies (Mozaffar et al., 2020; Zhang et al., 2021b). The decomposition of the PMF mass balance equations is simplified as follows (Norris et al., 2014):

$$x_{ij} = \sum_{k=1}^{p} g_{ik} \, f_{kj} + e_{ij} \qquad (1)$$

where x_{ij} is the mass concentration of species j measured in sample i; g_{ik} is the contribution of factor k to the sample i; f_{kj} represents the content of the jth species in factor k; e_{ij} is the residual of species j in sample i; p represents the number of factors. The fitting objective of the PMF model is to minimize the function Q to obtain the factor contributions and contours. The formula for Q is given in Eq. (2):

$$Q = \sum_{i=1}^{n} \sum_{j=1}^{m} \left[\frac{x_{ij} - \sum_{k=1}^{p} g_{ik} f_{kj}}{u_{ij}} \right]^2 \qquad (2)$$

196

197

198 where n and m denote the number of samples and VOC species, respectively.

199   Concentrations and uncertainty data are required for the PMF model. In this study,

200 the median concentration of a given species is used to replace missing values with an

201 uncertainty of four times of the median values; data less than the Method Detection

202 Limit (MDL) were replaced with half the MDL, with an uncertainty of 5/6 of the MDL;

203 and the uncertainty for values greater than the MDL was calculated using Eq. (3). In

204 Eq. (3), EF is error fraction, expressed as the precision of VOCs species, and the setting

205 range can be adjusted from 5 to 20% according to the concentration difference (Buzcu

206 et al., 2006; Song et al., 2007); and c_{ij} is the concentration of species j in sample i:

207
$$U_{ij} = \sqrt{\left(EF \times c_{ij} \right)^2 + (0.5 \times MDL)^2} \qquad (3)$$

208   when the concentration of VOCs in the species is less than the value of the

209 detection limit U_{ij} is calculated using Eq. (4):

210
$$U_{ij} = \left(\frac{5}{6} \right) MDL \qquad (4)$$

211   VOC species and concentration input into PMF were carefully selected to ensure

212 the accuracy of the PMF results. Species were excluded when over 25% of the samples

213 were missing or concentrations values were below the MDL (Gao et al., 2018); VOCs

214 with a short lifetime in the atmosphere were also excluded unless they are source-

215 relative species (Zhang et al., 2014; Shao et al., 2016). After that, retained VOC species

216 were categorized according to the signal-to-noise ratio (S/N) with S/N < 0.2 species

217 categorized as bad, 0.2 < S/N < 2 species categorized as weak; and S/N > 2 species

218 categorized as strong (Shao et al., 2016).

219   We used displacement of factor elements (DISP) to assess PMF modelling

220 uncertainty (for a description, see Paatero et al. (2014)). Q was less than 1% and no

221 swaps occurred for the small est dQ^{max} in DISP. Fpeak values from -2 to 2 were tested

222 to explore the rotational stability of the solutions. Q$_{true}$/Q$_{exp}$ is lowest when Fpeak = 0,

223 so we chose the PMF results for that case (Fig. S2a). After examining 3-8 factors, 20

224 base runs with 5 factors eventually selected to represent final result. We provide an

225 explanation of factor selection in the supplementary materials. Fig. S2(b) includes

226 Q$_{true}$/Q$_{exp}$, Q$_{robust}$/Q$_{exp}$ for factors 3-8. The slopes of these two ratios in changed at five

227 factors, and we found that five factors were more realistic after repeated comparisons
228 of the results at four, five and six factors.

2.3 SOA generation potential

230   The contributions of VOC species to SOAP were calculated based on the toluene
231 weighted mass contributions (TMC) method (Derwent et al., 2010). The methodology
232 for calculating SOAP is as follows:

233

234 $$SOAPF_i = \frac{VOCs\ component\ i\ to\ SOA\ mass\ concentration\ increments}{Toluene\ to\ SOA\ mass\ concentration\ increment} \times 100 \quad (5)$$

235

236     $SOAPF_i$ for each VOC is taken from the literature (Derwent et al., 2010). The
237 SOAP was estimated by multiplying the $SOAPF_i$ value by the concentration of
238 individual VOC species. The SOAP calculations through each VOC are as follows:

239

240 $$SOAP = \sum E_i \times SOAPF_i \quad (6)$$

241   E_i is the concentration of species i.

242

3. Results and discussion

### 3.1 Overview of variation in pollutants and meteorological parameters

246   Figure 1 shows the time series of meteorological parameters, TVOCs, O_3, NO_x,
247 SO_2, CO and $PM_{2.5}$ during the observed periods. Low WS and Temperature were found
248 with an average value of 1.3 ± 0.6 m/s and 5.0 ± 2.5 °C, respectively, during the entire
249 period, comparable with observations at the same site in 2021 (Lai et al., 2024). A total
250 of 62 days of valid data was acquired with the daily average concentration of $PM_{2.5}$
251 ranging from 53 to 239 $\mu g/m^3$, with the average value of 111 ± 45 $\mu g/m^3$. The
252 concentration of TVOCs ranged from 15.6 to 57.1 ppbv with an average of 36.1 ± 21.0
253 ppbv, higher than the same period in last year (27.9 ± 12.7 ppbv, Lai et al., 2024).
254 During the observation period, the average values of T, WS and RH were 5.0 ± 2.5 °C,
255 1.3 ± 0.6 m/s and $38.9 \pm 16.7\%$, respectively.
256   Previous studies have shown that meteorological factors such as low WS, high RH,

257   and low precipitation are responsible for the increase in $PM_{2.5}$ pollution in Zhengzhou

258   in winter (Duan et al., 2019). Our analysis of the correlation between different

259   pollutants and meteorological conditions during the pollution period showed that

260    $PM_{2.5}$, TVOCs and NO_x were positively correlated with relative humidity (Fig. S3),

261   which is consistent with the results of some previous studies (Wang et al., 2019). The

262   comparisons of average concentrations of different periods between different periods

263   are presented in Tables 1 and 2. In this study, the WS on clean days (1.4 ± 0.8 m/s)

264   was higher than in Case 1 (1.2 ± 0.9 m/s) and Case 2 (0.9 ± 0.7 m/s), while the RH

265   was lower by 26.2% and 12.5% compared to Case 1 and Case 2, respectively. These

266   findings indicate that high RH and low WS significantly influence the occurrence of

267   pollution during the observation period. WS, Temp and RH conditions during

268   infection and recovery periods were generally similar, and meteorology may also have

269   played a role in the differences between pollution events, but its specific influence was

270   not determined here. The average concentration of $PM_{2.5}$ during the recovery period

271   was 1.6 times the value during the infection period. Furthermore, the concentrations

272   of other pollutants including SO_2, NO_2, CO, and O_3 all showed a similar trend between

273   infection and recovery periods. The TVOC concentration during the recovery period

274   was 1.2 times the value during the infection period, showing an obvious increase trend

275   after resuming production. Decreased trends of air pollutants were found in other

276   studies before and after the outbreak of the novel coronavirus (COVID-19) in early

277   2020 (Qi et al., 2021; Wang et al., 2021).

278
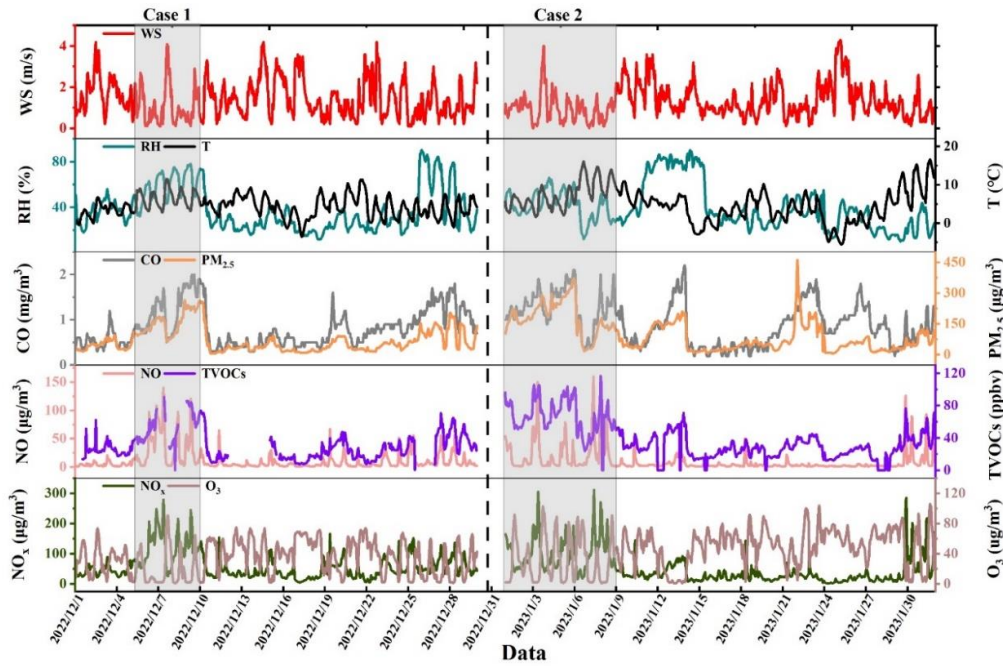
Fig. 1. Time series of WS, T, RH, CO, PM$_{2.5}$, NO, TVOCs, NO$_x$ and O$_3$ during the observation period.

The shadow section in Fig. 1 represents two haze pollution events during the monitoring period. A pollution event is determined when the daily average concentration of PM$_{2.5}$ exceeds 75 μg/m^3 (China's II-level standard) for at least three consecutive days. Case 1 (December 5 to December 10 with daily average PM$_{2.5}$ = 142.5 μg/m^3) and Case 2 (January 1 to January 8 with daily average PM$_{2.5}$ = 181.5 μg/m^3) were selected as they represent the pollution events in infection and recovery periods, respectively, due to their long duration and high pollution levels. Any day with a PM$_{2.5}$ concentration lower than 35 μg/m^3 (China's I-level standard) is considered as Clean day.
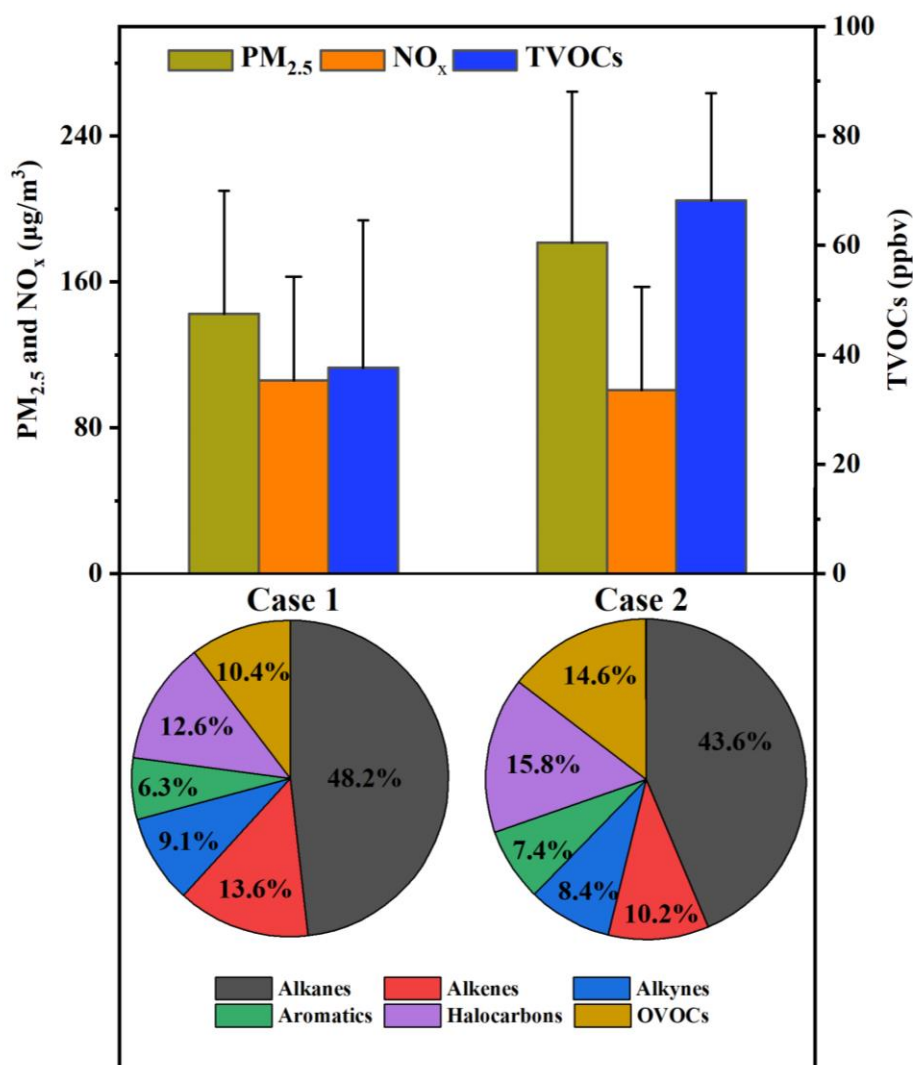
Fig. 2. The concentration of PM$_{2.5}$, NO$_x$, TVOCs and the composition ratio of VOCs in Case 1 and Case 2.

As for the two representative pollution processes (Case 1 during the infection period and Case 2 during the recovery period), the concentration of TVOCs in Case 1 and Case 2 were 48.4 ± 20.4 and 67.6 ± 19.6 ppbv (Fig. 2), respectively, increased by 63% and 188% compared with values during clean days. The average concentrations of PM$_{2.5}$ and TVOCs during Case 2 were 1.3 and 1.8 times the values in Case 1. The highest volume contributions of alkanes were found both in Case 1 (48%) and Case 2 (44%), consistent with the results in the Yangtze River Delta region (36-43%, Liu et al., 2023). While alkenes exhibited higher volume percentages of 13% in Case 1, followed by halogenated hydrocarbon (12%) and OVOCs (10%). Higher volume percentages of alkanes and alkenes in Case 1 were similar to the results in the gasoline evaporation site in winter (Niu et al., 2022). Equivalent volume contribution of halogenated hydrocarbon and OVOCs (15%) were found in Case 2, followed by alkenes (10%).

306   Although aromatic hydrocarbons have the lowest volumetric contribution (6% in Case

307   1 and 7% in Case 2), they show the largest increase from clean days to pollution.

308   Table 1 The average concentrations of meteorological parameters and pollutants during different

309   processes.

Category	Entire process (2022.12.1-2023.1.31)	Infection period (2022.12.1-2022.12.31)	Recovery period (2023.1.1-2023.1.31)	Case 1 (2022.12.5-2022.12.10)	Case 2 (2023.1.1-2023.1.8)	Clean Days
	N = 62 days	N = 31 days	N = 31 days	N = 6 days	N = 8 days	N = 8 days
WS (m/s)	1.3 ± 0.6	1.4 ± 0.6	1.3 ± 0.6	1.2 ± 0.9	0.9 ± 0.7	1.4 ± 0.8
T (°C)	5.0 ± 2.5	4.7 ± 1.7	5.4 ± 3.1	6.1 ± 2.2	7.4 ± 3.5	4.1 ± 3.0
RH (%)	38.9 ± 16.7	37.6 ± 15.5	40.2 ± 18.2	55.7 ± 14.7	42.0 ± 12.1	29.5 ± 18.1
TVOCs (ppbv)	36.1 ± 21.0	31.9 ± 18.1	39.8 ± 22.4	37.6 ± 27.0	68.2 ± 19.6	22.7 ± 11.1
SO_2 (μg/m^3)	11.4 ± 2.7	10.2 ± 2.8	12.7 ± 2.3	11.0 ± 3.7	16.2 ± 6.1	6.5 ± 2.5
NO_2 (μg/m^3)	47.2 ± 10.0	46.8 ± 8.6	47.8 ± 11.7	62.7 ± 20.5	65.0 ± 21.3	20.8 ± 15.9
CO (mg/m^3)	0.9 ± 0.2	0.8 ± 0.2	1.1 ± 0.2	1.2 ± 0.5	1.3 ± 0.4	0.5 ± 0.2
O_3 (μg/m^3)	34.9 ± 6.0	31.1 ± 4.5	39.0 ± 4.6	21.8 ± 23.7	32.5 ± 29.6	52.6 ± 18.4
$PM_{2.5}$ (μg/m^3)	111.5 ± 45.1	86.6 ± 34.6	138.3 ± 39.6	142.5 ± 67.4	181.5 ± 82.7	23.8 ± 16.8

310   Table 2 Concentration of VOC species during different processes (ppbv).

Category	Entire process	Infection period	Recovery period	Case 1	Case 2	Clean days
TVOCs	36.1 ± 21.0	31.9 ± 18.1	39.8 ± 22.4	48.4 ± 20.4	67.6 ± 19.6	17.5 ± 9.5
alkanes	16.8 ± 9.2	15.0 ± 8.4	18.4 ± 9.5	23.1 ± 10.0	29.5 ± 8.4	9.2 ± 5.6
alkenes	4.1 ± 2.7	3.8 ± 2.6	4.4 ± 2.7	6.5 ± 2.9	7.0 ± 2.6	1.7 ± 1.3
alkynes	3.1 ± 2.0	2.7 ± 1.7	3.4 ± 2.1	4.3 ± 2.0	5.8 ± 1.9	1.3 ± 0.8
aromatics	2.1 ± 2.0	1.8 ± 1.5	2.3 ± 2.2	3.0 ± 1.8	4.9 ± 2.8	0.7 ± 0.5
halogenated hydrocarbon	5.4 ± 3.3	4.4 ± 2.3	6.2 ± 3.8	6.0 ± 1.9	10.7 ± 3.6	2.7 ± 1.4
OVOCs	4.6 ± 3.2	3.5 ± 2.7	5.1 ± 3.5	5.0 ± 2.4	9.7 ± 2.8	1.9 ± 1.1

311 ## 3.2 Source Analysis of VOCs

312   Specific VOC ratios can be used for initial source identification of VOCs and

313   determination of photochemical ages of air masses (Monod et al., 2001; An et al., 2014;

314   Li et al., 2019). In this study, the ratios of toluene/benzene (T/B), isopentane/n-pentane,

315   isobutane/n-butane, and m/p-xylene/ethylbenzene (X/E) were selected to initially

316   identify the potential sources of VOCs (Fig. 3). Concentrations of selected pollutants

317   and ratios used are shown in Table S1.

318   The toluene-to-benzene ratio (T/B ratio) was widely used to assess the relative

319   importance of different sources. Specifically, T/B ratio with a value of 1.3-3.0 was

320   observed in vehicle emissions for vehicles with different fuel types (Schauer et al., 2002;

321   Wang et al., 2015). The reported T/B ratio for combustion processes was between 0.13

322   and 0.7 (Li et al., 2011; Wang et al., 2014). The mean value of T/B ratio for the entire

323   period was 1.0, with the majority of the data (99%) falling between 0.1 and 3.0 and

324   concentrated within the 0.7-1.3 range (49%). This suggests that both traffic emissions

325   and combustion may be significant sources of VOCs. It should be noted that this

326   analytical approach is not without limitations. The ratios observed here do not exclude

327   linear combinations from other sources. Consequently, an in-depth examination of the

328   sources of VOCs was conducted using the PMF model in the next section.

329   The isopentane/n-pentane concentration ratios of 0.6-0.8 represent mainly coal

330   combustion emissions, ratios of 0.8-0.9 represent LPG emissions, 2.2-3.8 represent

331   vehicle exhaust emissions, and 1.8-4.6 represent fuel evaporation (Conner et al., 1995;

332   Liu et al., 2008; Li et al., 2019). The sources of isopentane and n-pentane in this study

333   were intricate and multifaceted. The mean isopentane/n-pentane ratio was 1.4, with the

334   majority of data points (99%) falling within the range of 0.1-4.6, with a notable

335   concentration in the 0.8 to 1.8 interval. This indicates that pentane is susceptible to a

336   combination of LPG emissions and fuel evaporation. However, the proportion of

337   pentane may also be affected by a combination of coal combustion emissions and

338   vehicle exhaust.

339   Isobutane/n-butane concentration ratios of 0.2-0.3 represent vehicle emissions,

340   0.4-0.6 represent LPG usage, and 0.6-1.0 represent natural gas emissions (Russo et al.,

341   2010; Zheng et al., 2018). The mean isobutane/n-butane ratio in this study was 0.5, with

342   the majority of data points (99%) falling within the 0.4-0.6 range, indicating that VOCs

343   at the observation sites were significantly influenced by the use of LPG. (Shao et al.,

344   2016; Zeng et al., 2023). This result can also be caused by a combination of vehicle

345   exhaust and natural gas emissions.

346   The ratio of X/E can be used to infer the photochemical age of the air mass. X/E

347   ratios around 2.5-2.9 are typical of urban areas, indicating that VOCs are mainly from

348   the urban area (fresh air mass) (Kumar et al., 2018). When this ratio is significantly

349   lower than 3.0, it indicates that VOCs are mainly transported from distant sources

350   (aging air masses) (Kumar et al., 2018). The average X/E value in this study was 2.0

351   (Fig. 3(d)), indicating low photochemical activity and aging of the air mass at the

352 observation site. Potential source analyses also indicate that air masses are affected by

353 long-range transport (Fig. S4).
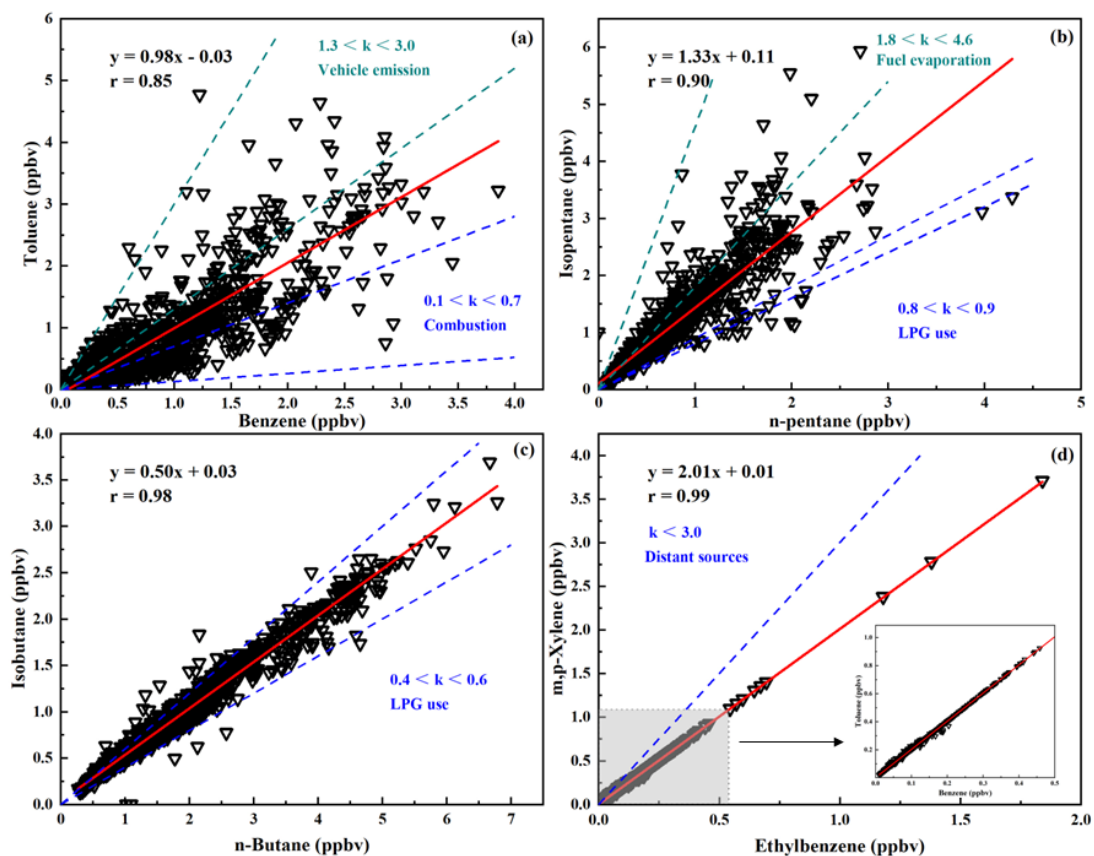
354

355 Fig. 3. Correlation analysis between specific VOC species.

356 Figure 4 shows the chemical profiles of individual VOCs resolved by the PMF

357 model during the entire observation period. These five factors eventually selected as

358 potential sources for the observed VOCs are: (1) Fuel evaporation; (2) Solvent usage;

359 (3) Vehicular emission; (4) Industrial source; and (5) Combustion. These 5 factors have

360 been commonly reported before, e.g., in Shijiazhuang, northern China (Guan et al, 2023)

361 and in Beijing (Cui et al., 2022).

362 Alkanes of C4-C6 substances were predominant in factor 1, including 2-

363 methylpentane, 3-methylpentane, isobutane, n-butane, isopentane and n-pentane from

364 oil and gas (Xiong et al., 2020). Fig. S5 shows that emissions from this source peak at

365 midday, when fuel volatilization is high, The CPF plot shows that south-east is the

366 dominant direction at wind speeds of less than 2 m/s (Fig. 5a). Therefore, factor 1 was

367 identified as the source of oil and gas volatilization.

368 The contribution of benzene, toluene, methylene chloride, 1,2-dichloroethane and

369 ethyl acetate was high in factor 2. It has been shown that benzene, toluene, ethylbenzene,

370 and xylene is an important component in the use of solvents (Li et al., 2015); methylene

371 chloride is often used as a chemical solvent, while esters are mostly used as industrial

372 solvents or adhesives (Li et al., 2015). Factor 2 is determined to be solvent usage source.

373 The CPF plot shows that due east is the main emission direction at wind speeds less

374 than 2 m/s and southeast is the main source at wind speeds greater than 2 m/s (Fig. 5b).

375 Factor 3 contains predominantly C3-C8 alkanes, olefins and alkynes, and

376 relatively high concentrations of benzene. These substances are usually emitted by

377 industrial processes (Shao et al., 2016), so Factor 4 is defined as an industrial source.

378 The CPF plots indicate that a local source at low wind speeds is the dominant sources

379 (Fig. 5c).

380 Factor 4 is characterized by relatively high levels of C2-C6 low-carbon alkanes

381 (ethane, propane, isopentane, n-pentane, isobutane and n-butane), olefins (ethylene and

382 propylene), and benzene and toluene, which are important automotive exhaust tracers

383 (Song et al., 2021; Zhang et al., 2021b). Ethylene and propylene are important

384 components derived from vehicle-related activities. Previous studies of VOCs in

385 Zhengzhou have shown a high percentage of VOCs emitted from gasoline vehicles,

386 with the main source of alkanes being on-road mobile sources (Bai et al., 2020). The

387 daily variation of this source in Fig. S5 shows a bimodal trend, with peaks occurring in

388 the morning and evening peaks of traffic, consistent with motor vehicle emissions. Fig.

389 5d shows that this source is mainly from the west where wind speeds are below 2 m/s,

390 and in this direction, there are a number of urban arterial roads with high traffic volumes.

391 Therefore, factor 4 was defined as vehicular emission source.

392 The highest contribution to factor 5 is chloromethane (62%). Benzene (46%) and

393 acetylene (41%) also contribute highly to factor 5. Chloromethane is the key tracer for

394 biomass combustion and acetylene is the key tracer for coal combustion (Xiong et al.,

395 2020). Therefore, factor 5 is defined as a combustion source. The CPF plot shows that

396 at wind speeds below 2 m/s, the north-east direction is the dominant source direction

397 (Fig. 5e).
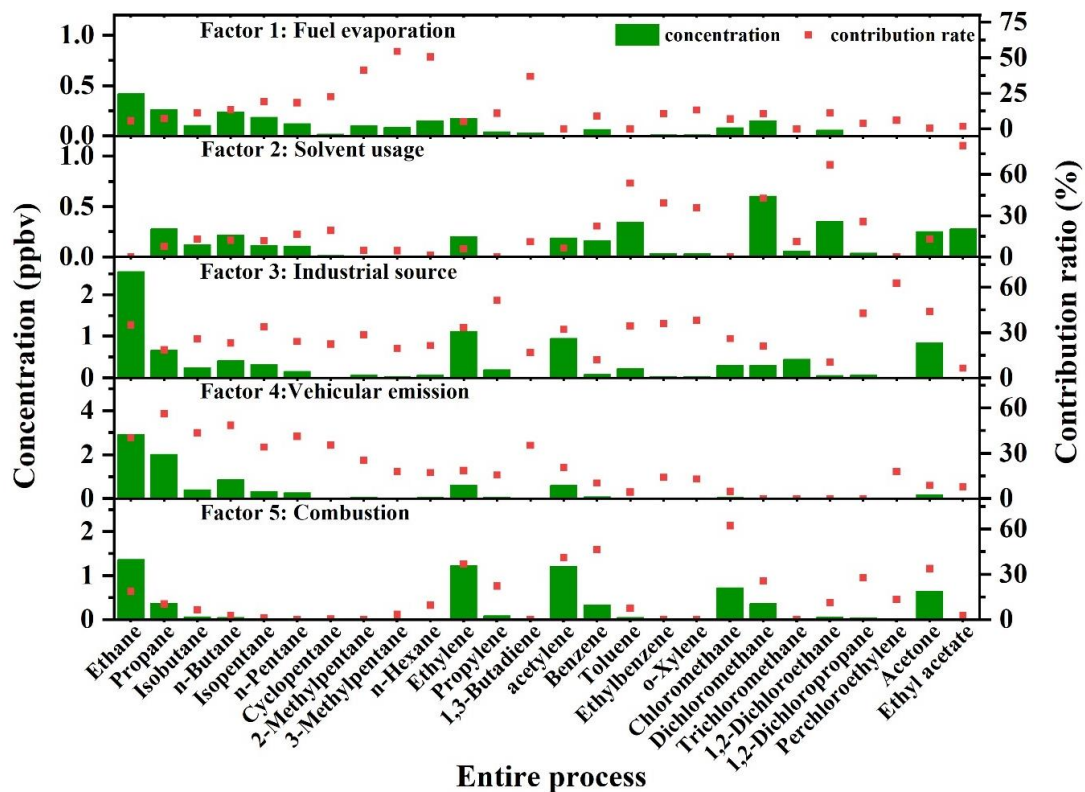
398

399   Fig. 4. Concentration of VOC species in each factor and contribution to each source.
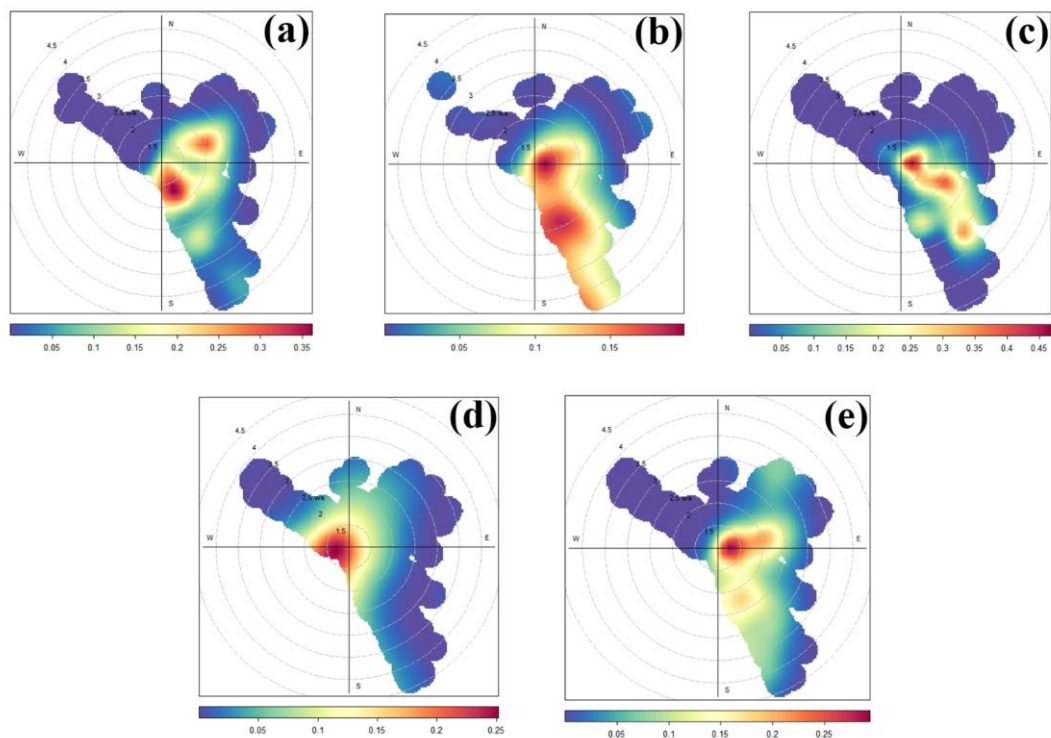

400

401   Fig. 5. CPF plots of five VOCs sources obtained using the PMF model.

Fig. S6 compares the differences in PMF source profiles between the Omicron infection period and the recovery period, as well as between the pollution day and the clean day. We present the concentrations of the five main VOCs in all five factors in Table S2. Ethane (vehicular emission), 2-methylpentane (fuel evaporation), benzene (industry source), chloromethane (combustion), and ethyl acetate (solvent usage) were selected as tracers for five sources. Ethane concentration in Case 2 (5.9 ppbv) is much higher than in other processes, and ethane concentration during the recovery period (3.4 ppbv) is also higher than during the infection period (2.4 ppbv), which may to some extent reflect increased vehicular emissions during the recovery period.

Concentrations of most species were significantly higher during the recovery period than during the infection period. The representative pollution processes in both periods showed the same results as well, with a 79% higher concentration of TVOCs in Case 2 (65.1 ppbv) compared to Case 1 (36.3 ppbv) (Fig. 6). While in Case 1 industry was the dominant source of VOCs, by Case 2 motorized sources reached a concentration value of 21.2 ppbv, accounting for 33% of the observed VOCs, and became the dominant source of emissions. This is consistent with the fact that people's mobility activities have increased after the epidemic has entered the recovery period. As a group of VOCs species with the highest concentration share, ethane and propane contributed more to the clean days motor vehicle source than other processes, which also resulted in a 34% clean days motor vehicle source share.
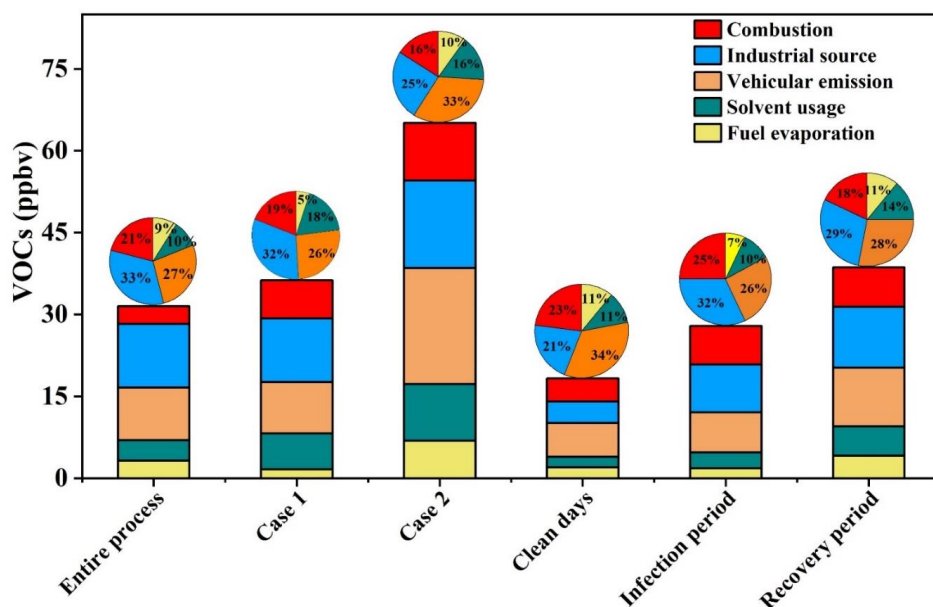
Fig. 6. Contribution of each to VOCs for different processes.

3.3 SOAP

VOCs are estimated to contribute about 16−30% or more of PM$_{2.5}$ by mass through SOA production (Huang et al., 2014). Therefore, by calculating the SOAP value, the influence of different sources on PM$_{2.5}$ production can be reflected to a certain extent.

We have included quantitative analysis for SOAP as well. Fig. 7 shows the SOAP concentrations and contribution rates of the top ten species throughout the entire process, during two pollution processes, and clean days. The top ten species all reached close to 100% of the total SOAP contribution, with Case 1 reaching 98%. In each process, the composition of the top ten substances is essentially the same. Aromatic hydrocarbons contributed the most, with BTEX always occupying the top five positions and toluene the most. The SOAP values of the top ten contributing species for the two polluting processes are shown in Tables S3 and S4. Toluene, the highest contributing species, reached a SOAP value of 49.4 μg/m^3 in the most polluted Case 2, which was 3.2 times higher than the SOAP sum of all species on the clean day (15.5 μg/m^3). The SOAP value for Case 1, which is also a contaminated process, was 67 μg/m^3, and the main species (m/xylene: 9.8 μg/m^3, benzene: 8.5 μg/m^3) including toluene (34.6 μg/m^3) were lower than those for Case 2 (m/xylene: 19.4 μg/m^3, benzene: 13.4 μg/m^3).
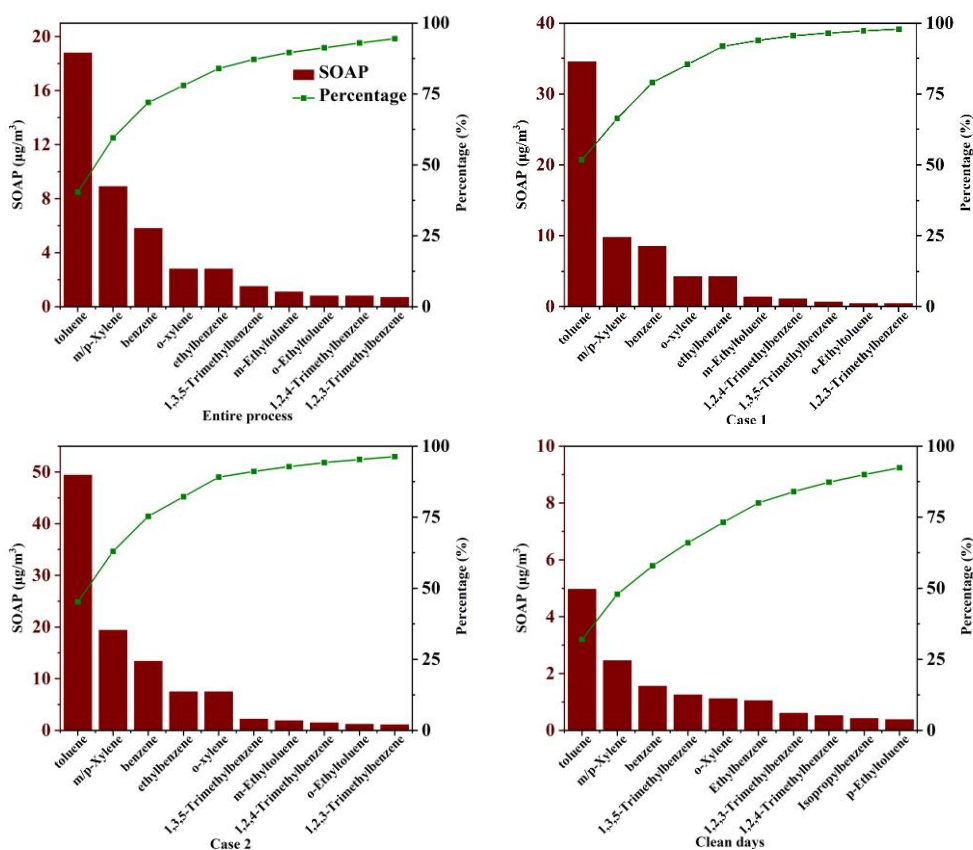
445   Figure 8 shows the SOAP calculated after source resolution of the two pollution

446   processes by PMF for clean days, respectively. In Case 1, industrial source is the

447   dominant source with a contribution ratio of 63%. In Case 2, the pollution sources

448   exhibit a more evenly distributed contribution, where the solvent usage and fuel

449   evaporation sources emerge as the primary contributors to SOAP, with their respective

450   contribution levels rising to 32% and 26%. Case 1 was during the infection period,

451   when social activities had not yet returned to normal. In Case 2, when society had

452   basically returned to normal, the increase in emissions from various sources resulted in

453   a more balanced distribution of SOAP contributions and caused more severe $PM_{2.5}$

454   pollution. In addition, a few days before Case 2, the Zhengzhou Municipal People's

455   Government   initiated   the   Heavy   Pollution   Weather   Level   II   response

456   (https://sthjj.zhengzhou.gov.cn/tzgg/7037130.jhtml) and introduced control measures

457   for emissions from industrial and mobile sources, which resulted in a significant

458   reduction of SOAP levels from industrial and motorized sources in Case 2. The clean

459   day result with a SOAP of 8.8 $\mu g/m^3$ also indicates that industrial and solvent usage

460   sources are the most dominant SOAP sources. The primary sources of aromatic

461   compounds, which are the most significant contributors to SOAP, are solvent usage and

462   industrial process emissions. This finding aligns with the results of other studies (Wu

463   et al., 2017). Consequently, it is imperative to implement measures to reduce $PM_{2.5}$

464   pollution by regulating emissions from industrial and solvent usage sources.

465
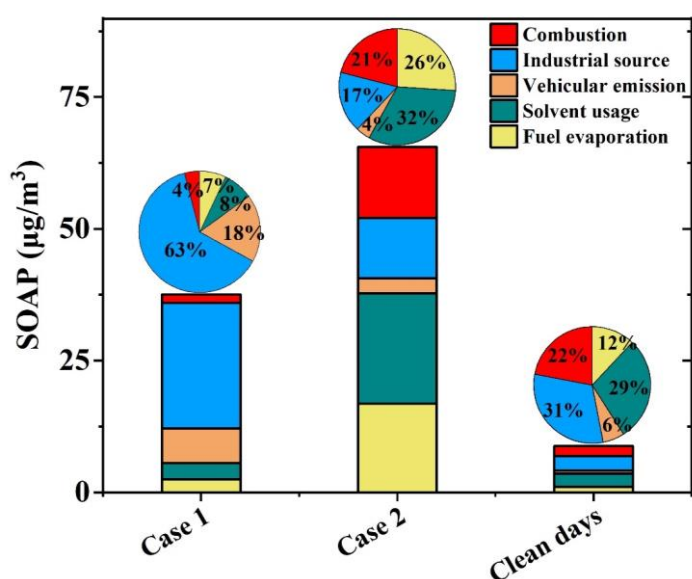
466   Fig. 8. SOAP value and contribution ratio of each process

467

4. Conclusions

Continuous observation of VOCs during the infection of the Omicron epidemic was carried out at an urban site in polluted Zhengzhou from December 1, 2022, to January 31, 2023. The daily average concentration of $PM_{2.5}$ ranged from 53.5 to 239.4 $\mu g/m^3$ with an average value of 111.5 ± 45.1 $\mu g/m^3$ during the whole period. The concentration of TVOCs ranged from 15.6 to 57.1 ppbv with an average of 36.1 ± 21.0 ppbv, higher than the same period in last year (27.9 ± 12.7 ppbv, Lai et al., 2024). Two representative contamination processes were identified (Case 1 during the infection period and Case 2 during the recovery period). While the meteorological conditions of the two pollution processes are relatively similar, the specific impacts caused thereby have yet to be determined. The concentration of TVOCs in Case 1 and Case 2 were 48.4 ± 20.4 and 67.6 ± 19.6 ppbv, respectively, increased by 63% and 188% compared with values during clean days. The average concentrations of $PM_{2.5}$ and TVOCs during Case 2 were 1.3 and 1.8 times of the values in Case 1. This is consistent with the observed increase in pollutant emissions following the return to normal social life from the period of Omicron infection. The highest volume contributions of alkanes were found both in Case 1 (48%) and Case 2 (44%). Though the volume contribution of aromatics were the lowest (6% in Case 1 and 7% in Case 2), the highest increase ratio was found from clean days to polluted episodes. Low wind speed and high humidity were the main meteorological reasons for the occurrence of pollution. Analyzing the sources of VOCs revealed that VOCs were found to be affected by a combination of local emissions and regional transport. The primary sources of atmospheric VOCs in Zhengzhou were identified as industrial emissions (32%), vehicle emissions (27%), and combustion (21%). Significant discrepancies were observed in the sources of VOCs between the two pollution processes. In Case 1, industrial emissions constituted the primary source of VOCs, accounting for 32% of the total VOC concentration. In contrast, in Case 2, the proportion of vehicle emissions increased to 33%, representing the primary source of VOCs.

A further analysis of the effect of VOCs on SOA generation reveals that aromatic compounds are the primary contributors to SOAP, with BTEX being the predominant contributor throughout the period. The SOAP values reached 37.6 and 65.6 $\mu g/m^3$ in Case 1 and Case 2, respectively. In Case 1, the greatest contribution to SOAP was made by industrial sources (63%, 23.8 $\mu g/m^3$), while vehicular sources, which constituted the

second most important source, accounted for only 18%. In Case 2, the contribution of each VOC source was more evenly distributed, with solvent use sources and fuel evaporation sources representing the primary contributors to SOAP, accounting for 32% (20.9 μg/m³) and 26% (16.8 μg/m³), respectively. The SOAP result for the clean day was 8.8 μg/m³, with industrial sources and solvent use still being the primary contributors. Therefore, the industrial and solvent use sectors are the predominant sources of pollutants during this observation. The aforementioned results substantiate the considerable impact of elevated emissions from all sources on the exacerbation of pollution following the conclusion of the Omicron infection.

Author contribution:

Bowen Zhang: Data curation, Methodology, Formal analysis, Writing Original Draft.

Dong Zhang: Data curation, Formal analysis, Review & Editing.

Zhe Dong: Data curation, Formal analysis, Review & Editing.

Xinshuai Song: Data curation, Formal analysis.

Ruiqin Zhang: Supervision, Writing-Review & Editing, Funding acquisition.

Xiao Li: Formal analysis, Investigation, Supervision, Writing-Review & Editing.

Competing interests:

The contact author has declared that none of the authors has any competing interests.

References

An, J., Zhu, B., Wang, H., Li, Y., Lin, X., and Yang, H.: Characteristics and source apportionment of VOCs measured in an industrial area of Nanjing, Yangtze River Delta, China, Atmospheric Environment, 97, 206-214, https://doi.org/10.1016/j.atmosenv.2014.08.021, 2014.

Bai, L., Lu, X., Yin, S., Zhang, H., Ma, S., Wang, C., Li, Y., and Zhang, R.: A recent emission inventory of multiple air pollutant, $PM_{2.5}$ chemical species and its spatial-temporal characteristics in central China, Journal of Cleaner Production, 269,

531 122114, https://doi.org/10.1016/j.jclepro.2020.122114, 2020.

532 Buzcu, B. and Fraser, M. P.: Source identification and apportionment of volatile

533 organic compounds in Houston, TX, Atmospheric Environment, 40, 2385-2400,

534 https://doi.org/10.1016/j.atmosenv.2005.12.020, 2006.

535 Conner, T. L., Lonneman, W. A., Seila, R.L.: Transportation-related volatile

536 hydrocarbon source profiles measured in atlanta, Journal of the Air & Waste

537 Management Association, 45 (5), 383-394,

538 https://doi.org/10.1080/10473289.1995.10467370, 1995.

539 Cui, L., Wu, D., Wang, S., Xu, Q., Hu, R., and Hao, J.: Measurement report:

540 Ambient volatile organic compound (VOC) pollution in urban Beijing: characteristics,

541 sources, and implications for pollution control, Atmospheric Chemistry and Physics,

542 22, 11931-11944, https://doi.org/10.5194/acp-22-11931-2022, 2022.

543 Derwent, R. G., Jenkin, M. E., Utembe, S. R., Shallcross, D. E., Murrells, T. P.,

544 and Passant, N. R.: Secondary organic aerosol formation from a large number of

545 reactive man-made organic compounds, Science of the Total Environment, 408, 3374-

546 3381, https://doi.org/10.1016/j.scitotenv.2010.04.013, 2010.

547 Duan, S., Jiang, N., Yang, L., Zhang, R.: Transport Pathways and Potential Sources

548 of $PM_{2.5}$ During the Winter in Zhengzhou, Environmental Science, Jan 8;40(1):86-93,

549 https://doi.org/10.13227/j.hjkx.201805187, 2019.

550 Gao, J., Zhang, J., Li, H., Li, L., Xu, L., Zhang, Y., Wang, Z., Wang, X., Zhang,

551 W., Chen, Y., Cheng, X., Zhang, H., Peng, L., Chai, F., and Wei, Y.: Comparative study

552 of volatile organic compounds in ambient air using observed mixing ratios and initial

553 mixing ratios taking chemical loss into account – A case study in a typical urban area

554 in Beijing, Science of the Total Environment, 628-629, 791-804,

555 https://doi.org/10.1016/j.scitotenv.2018.01.175, 2018.

556 Guan, Y., Liu, X., Zheng, Z., Dai, Y., Du, G., Han, J., Hou, L. a., and Duan, E.:

557 Summer O_3 pollution cycle characteristics and VOCs sources in a central city of

558 Beijing-Tianjin-Hebei area, China, Environmental Pollution, 323, 121293,

559 https://doi.org/10.1016/j.envpol.2023.121293, 2023.

560 Huang, R., Zhang, Y., Bozzetti, C. et al.: High secondary aerosol contribution to p

561 articulate pollution during haze events in China, Nature, 514 (7521), 218−22, https://d

562 oi.org/10.1038/nature13774, 2014.

563 Hui, L., Liu, X., Tan, Q., Feng, M., An, J., Qu, Y., Zhang, Y., Deng, Y., Zhai, R., a

564 nd Wang, Z.: VOC characteristics, chemical reactivity and sources in urban Wuhan, ce

565 ntral China, Atmospheric Environment, 224, 117340, https://doi.org/10.1016/j.atmose

566 nv.2020.117340, 2020.

567   Jensen, A., Liu, Z., Tan, W., Dix, B., Chen, T., Koss, A., Zhu, L., Li, L., de Gouw,

568 J.: Measurements of volatile organic compounds during the COVID-19 lockdown in

569 Changzhou, China, Geophysical research letters, 48(20), https://doi.org/10.1029/2021

570 GL095560, 2021.

571   Jiang, N., Hao, X., Hao, Q., Wei, Y., Zhang, Y., Lyu, Z., Zhang, R.: Changes in se

572 condary inorganic ions in $PM_{2.5}$ at different pollution stages before and after COVID-1

573 9 control, Environmental Science, 44(5), 2430-2440, https://doi.org/10.13227/j.hjkx.2

574 02206170, 2023.

575   Kumar, A., Singh, D., Kumar, K., Singh, B. B., and Jain, V. K.: Distribution of

576 VOCs in urban and rural atmospheres of subtropical India: Temporal variation, source

577 attribution, ratios, OFP and risk assessment, Science of the Total Environment, 613-614,

578 492-501, https://doi.org/10.1016/j.scitotenv.2017.09.096, 2018.

579   Lai, M., Zhang, D., Yin, S., Song, X., and Zhang, R.: Pollution characteristics,

580 source apportionment and activity analysis of atmospheric VOCs during winter and

581 summer pollution in Zhengzhou City, Environmental Science, 4108, 3500-3510,

582 https://doi.org/10.13227/j.hjkx.202001133, 2024.

583   Li, B., Ho, S. S. H., Gong, S., Ni, J., Li, H., Han, L., Yang, Y., Qi, Y., and Zhao,

584 D.: Characterization of VOCs and their related atmospheric processes in a central

585 Chinese city during severe ozone pollution periods, Atmospheric Chemistry and

586 Physics, 19, 617-638, https://doi.org/10.5194/acp-19-617-2019, 2019.

587   Li, J., Deng, S., Tohti, A., Li, G., Yi, X., Lu, Z., Liu, J., and Zhang, S.: Spatial

588 characteristics of VOCs and their ozone and secondary organic aerosol formation

589 potentials in autumn and winter in the Guanzhong Plain, China, Environmental

590 Research, 211, 113036, https://doi.org/10.1016/j.envres.2022.113036, 2022.

591   Li, J., Xie, S. D., Zeng, L. M., Li, L. Y., Li, Y. Q., and Wu, R. R.: Characterization

592 of ambient volatile organic compounds and their sources in Beijing, before, during, and

593 after Asia-Pacific Economic Cooperation China 2014, Atmospheric Chemistry and

594 Physics, 15, 7945-7959, https://doi.org/10.5194/acp-15-7945-2015, 2015.

595   Li, J., Lu, K., Lv, W., Li, J., Zhong, L., Ou, Y., Chen, D., Huang, X., and Zhang,

596 Y.: Fast increasing of surface ozone concentrations in Pearl River Delta characterized

597 by a regional air quality monitoring network during 2006–2011, Journal of

598 Environmental Sciences, 26, 23-36, https://doi.org/10.1016/S1001-0742(13)60377-0,

599　2014.

600　Liu, Y., Li, X., Tang, G., Wang, L., Lv, B., Guo, X., and Wang, Y.: Secondary
601　organic aerosols in Jinan, an urban site in North China: Significant anthropogenic
602　contributions to heavy pollution, Journal of Environmental Sciences, 80, 107-115,
603　https://doi.org/10.1016/j.jes.2018.11.009, 2019.

604　Liu, Y., Shao, M., Fu, L., Lu, S., Zeng, L., and Tang, D.: Source profiles of volatile
605　organic compounds (VOCs) measured in China: Part I, Atmospheric Environment, 42,
606　6247-6260, https://doi.org/10.1016/j.atmosenv.2008.01.070, 2008.

607　Liu, Y., Song, M., Liu, X., Zhang, Y., Hui, L., Kong, L., Zhang, Y., Zhang, C., Qu,
608　Y., An, J., Ma, D., Tan, Q., and Feng, M.: Characterization and sources of volatile
609　organic compounds (VOCs) and their related changes during ozone pollution days in
610　2016 in Beijing, China, Environmental Pollution, 257, 113599,
611　https://doi.org/10.1016/j.envpol.2019.113599, 2020.

612　Liu, Z., Hu, K., Zhang, K., Zhu, S., Wang, M., and Li, L.: VOCs sources and roles
613　in O_3 formation in the central Yangtze River Delta region of China, Atmospheric
614　Environment, 302, https://doi.org/10.1016/j.atmosenv.2023.119755, 2023.

615　Li, X., Wang, S., Hao, J.: Characteristics of volatile organic compounds (VOCs)
616　emitted from biofuel combustion in China, Environmental Science, 32, 3515-3521,
617　2011.

618　Li, Y., Yin, S., Zhang R., Yu, S., Yang, J., and Zhang, D.: Characteristics and source
619　apportionment of atmospheric VOCs at different pollution levels in winter in an urban
620　area in Zhengzhou, Environmental Science, 4108, 3500-3510,
621　https://doi.org/10.13227/j.hjkx.202001133, 2020.

622　Ma, Q., Wang, W., Wu, Y., Wang, F., Jin, L., Song, Y., Han, Y., Zhang, R., Zhang,
623　D.: Haze caused by NO_x oxidation under restricted residential and industrial activities
624　in a mega city in the south of North China Plain, Chemosphere, Volume 305, 135489,
625　https://doi.org/10.1016/j.chemosphere.2022.135489, 2022.

626　Merino, M., Marinescu, M., Cascajo, A., Carretero, J., Singh, D.: Evaluating the
627　spread of Omicron COVID-19 variant in Spain, Future Generation Computer Systems,
628　149, 547-561, https://doi.org/10.1016/j.future.2023.07.025, 2023.

629　Monod, A., Sive, B. C., Avino, P., Chen, T., Blake, D. R., and Sherwood Rowland,
630　F.: Monoaromatic compounds in ambient air of various cities: a focus on correlations
631　between the xylenes and ethylbenzene, Atmospheric Environment, 35, 135-149,
632　https://doi.org/10.1016/S1352-2310(00)00274-0, 2001.

Mozaffar, A., Zhang, Y.-L., Fan, M., Cao, F., and Lin, Y.-C.: Characteristics of summertime ambient VOCs and their contributions to O_3 and SOA formation in a suburban area of Nanjing, China, Atmospheric Research, 240, 104923, https://doi.org/10.1016/j.atmosres.2020.104923, 2020.

Mu, L., Feng, C., Li, Y., Li, X., Liu, T., Jiang, X., Liu, Z., Bai, H., and Liu, X.: Emission factors and source profiles of VOCs emitted from coke production in Shanxi, China, Environmental Pollution, 335, 122373, https://doi.org/10.1016/j.envpol.2023.122373, 2023.

Niu, Y., Yan, Y., Chai, J., Zhang, X., Xu, Y., Duan, X., Wu, J., and Peng, L.: Effects of regional transport from different potential pollution areas on volatile organic compounds (VOCs) in Northern Beijing during non-heating and heating periods, Science of the Total Environment, 836, 155465, https://doi.org/10.1016/j.scitotenv.2022.155465, 2022.

Norris, G., Duvall, R., Brown, S., Bai. S. EPA Positive Matrix Factorization (PMF) 5.0 Fundamentals and User Guide. U.S. Environmental Protection Agency, Washington, DC, EPA/600/R-14/108 (NTIS PB2015-105147), 2014.

Paatero, P., Eberly, S., Brown, S. G., Norris, G. A.: Methods for estimating uncertainty in factor analytic solutions, Atmospheric Measurement Techniques, Volume 7, 781-797, https://doi.org/10.5194/amt-7-781-2014, 2014.

Pei, C., Yang, W., Zhang, Y., Song, W., Xiao, S., Wang, J., Zhang, J., Zhang, T., Chen, D., Wang, Y., Chen, Y., Wang, X.: Decrease in ambient volatile organic compounds during the COVID-19 lockdown period in the Pearl River Delta region, south China, Science of The Total Environment, 823, 153720, https://doi.org/10.1016/j.scitotenv.2022.153720, 2022.

Petersen, M. S., Í Kongsstovu, S., Eliasen, E. H., Larsen, S., Hansen, J. L., Vest, N., Dahl, M. M., Christiansen, D. H., Møller, L. F., & Kristiansen, M. F.: Clinical characteristics of the Omicron variant - results from a Nationwide Symptoms Survey in the Faroe Islands, International Journal of Infectious Diseases, 122, 636–643, https://doi.org/10.1016/j.ijid.2022.07.005, 2022.

Qi, J., Mo, Z., Yuan, B., Huang, S., Huangfu, Y., Wang, Z., Li, X., Yang, S., Wang, W., Zhao, Y., Wang, X., Wang, W., Liu, K., and Shao, M.: An observation approach in evaluation of ozone production to precursor changes during the COVID-19 lockdown, Atmospheric Environment, 262, 118618, https://doi.org/10.1016/j.atmosenv.2021.118618, 2021.

Russo, R. S., Zhou, Y., White, M. L., Mao, H., Talbot, R., and Sive, B. C.: Multi-year (2004–2008) record of nonmethane hydrocarbons and halocarbons in New England: seasonal variations and regional sources, Atmospheric Chemistry and Physics, 10, 4909-4929, https://doi.org/10.5194/acp-10-4909-2010, 2010.

Sahu, L. K., Tripathi, N., Gupta, M., Singh, V., Yadav, R., Patel, K.: Impact of COVID-19 Pandemic lockdown in ambient concentrations of aromatic volatile organic compounds in a metropolitan city of western India, Journal of geophysical research, Atmospheres : JGR, 127(6), https://doi.org/10.1029/2022JD036628, 2022.

Schauer, J., Kleeman, M., Cass, G., Simoneit, B.: Measurement of emissions from air pollution sources.5. C_1-C_{32} organic compounds from gasoline-powered motor vehicles, Environmental Science & Technology, 36, 1169-1180, https://doi.org/10.1021/es0108077, 2002.

Shao, P., An, J., Xin, J., Wu, F., Wang, J., Ji, D., and Wang, Y.: Source apportionment of VOCs and the contribution to photochemical ozone formation during summer in the typical industrial area in the Yangtze River Delta, China, Atmospheric Research, 176-177, 64-74, https://doi.org/10.1016/j.atmosres.2016.02.015, 2016.

Shi, Y., Liu, C., Zhang, B., Simayi, M., Xi, Z., Ren, J., and Xie, S.: Accurate identification of key VOCs sources contributing to O_3 formation along the Liaodong Bay based on emission inventories and ambient observations, Science of the Total Environment, 844, 156998, 10.1016/j.scitotenv.2022.156998, 2022.

Singh, B., Sohrab, S., Athar, M., Alandijany, T., Kumari, S., Nair, A., Kumari, S., Mehra, K., Chowdhary, K., Rahman, S., Azhar, E.: Substantial changes in selected volatile organic compounds (VOCs) and associations with health risk assessments in industrial areas during the COVID-19 Pandemic, Toxics, 11, 165, https://doi.org/10.3390/toxics11020165, 2023a.

Singh, B., Singh, M., Ulman, Y., Sharma, U., Pradhan, R., Sahoo, J., Padhi, S., Chandra, P., Koul, M., Tripathi, P., Kumar, D., Masih, J.: Distribution and temporal variation of total volatile organic compounds concentrations associated with health risk in Punjab, India, Case Studies in Chemical and Environmental Engineering, 8, 100417, https://doi.org/10.1016/j.cscee.2023.100417, 2023b.

Song, M., Li, X., Yang, S., Yu, X., Zhou, S., Yang, Y., Chen, S., Dong, H., Liao, K., Chen, Q., Lu, K., Zhang, N., Cao, J., Zeng, L., and Zhang, Y.: Spatiotemporal variation, sources, and secondary transformation potential of volatile organic compounds in Xi'an, China, Atmospheric Chemistry and Physics, 21, 4939-4958,

701 https://doi.org/10.5194/acp-21-4939-2021, 2021.

702 Song, X., Zhang, D., Li, X., Lu, X., Wang, M., Zhang, B., Zhang, R.: Simultaneous

703 observations of peroxyacetyl nitrate and ozone in Central China during static

704 management of COVID-19: Regional transport and thermal decomposition,

705 Atmospheric Research, Volume 294, 106958,

706 https://doi.org/10.1016/j.atmosres.2023.106958, 2023.

707 Song, Y., Shao, M., Liu, Y., Lu, S., Kuster, W., Goldan, P., and Xie, S.: Source

708 apportionment of ambient volatile organic compounds in Beijing, Environmental

709 Science & Technology, 41, 4348-4353, https://doi.org/10.1021/es0625982, 2007.

710 Wang, H., Li, J., Peng, Y., Zhang, M., Che, H., Zhang, X.: The impacts of the

711 meteorology features on $PM_{2.5}$ levels during a severe haze episode in central-east China,

712 Atmospheric Environment, Volume 197, Pages 177-189, ISSN 1352-2310,

713 https://doi.org/10.1016/j.atmosenv.2018.10.001, 2019.

714 Wang, H., Wang, Q., Chen, J. Chen, C., Huang, C., Qiao, L. Lou, S., Lu, J.: Do

715 vehicular emissions dominate the source of C6–C8 aromatics in the megacity Shanghai

716 of eastern China?, Environmental Science, 27, 290-297, https://doi.org/10.

717 1016/j.jes.2014.05.033, 2015.

718 Wang, M., Lu, S., Shao, M., Zeng, L., Zheng, J., Xie, F., Lin, H., Hu, K., and Lu,

719 X.: Impact of COVID-19 lockdown on ambient levels and sources of volatile organic

720 compounds (VOCs) in Nanjing, China, Science of the Total Environment, 757, 143823,

721 https://doi.org/10.1016/j.scitotenv.2020.143823, 2021.

722 Wang, M., Zeng, L., Lu, S., Shao, M., Liu, X., Yu, X., Chen, W., Yuan, B., Zhang,

723 Q., Hu, M., & Zhang, Z.: Development and validation of a cryogen-free automatic gas

724 chromatograph system (GC-MS/FID) for online measurements of volatile organic

725 compounds, Analytical Methods, 6, 9424, https://doi.org/10.1039/C4AY01855A, 2014.

726 Wang, T., Xue, L., Brimblecombe, P., Lam, Y. F., Li, L., and Zhang, L.: Ozone

727 pollution in China: A review of concentrations, meteorological influences, chemical

728 precursors, and effects, Science of the Total Environment, 575, 1582-1596,

729 https://doi.org/10.1016/j.scitotenv.2016.10.081, 2017.

730 Wu, R., Li, J., Hao, Y., Li, Y., Zeng, L., and Xie, S.: Evolution process and sources

731 of ambient volatile organic compounds during a severe haze event in Beijing, China,

732 Science of the Total Environment, 560-561, 62-72,

733 https://doi.org/10.1016/j.scitotenv.2016.04.030, 2016.

734 Wu, W., Zhao, B., Wang, S., and Hao, J.: Ozone and secondary organic aerosol

formation potential from anthropogenic volatile organic compounds emissions in China, Journal of Environmental Sciences, 53, 224-237, https://doi.org/10.1016/j.jes.2016.03.025, 2017.

Xiong, Y., Zhou, J., Xing, Z., and Du, K.: Optimization of a volatile organic compound control strategy in an oil industry center in Canada by evaluating ozone and secondary organic aerosol formation potential, Environmental Research, 191, 110217, https://doi.org/10.1016/j.envres.2020.110217, 2020.

Yun, L., Li, C., Zhang, M., He, L. and Guo, J.: Pollution characteristics and sources of atmospheric VOCs in the coastal background area of the Pearl River Delta, Environmental Science, 4191-4201, https://doi.org/10.13227/j.hjkx.202101155, 2021.

Zeng, X., Han, M., Ren, G., Liu, G., Wang, X., Du, K., Zhang, X., and Lin, H.: A comprehensive investigation on source apportionment and multi-directional regional transport of volatile organic compounds and ozone in urban Zhengzhou, Chemosphere, 334, 139001, https://doi.org/10.1016/j.chemosphere.2023.139001, 2023.

Zhang, C., Liu, X., Zhang, Y., Tan, Q., Feng, M., Qu, Y., An, J., Deng, Y., Zhai, R., Wang, Z., Cheng, N., and Zha, S.: Characteristics, source apportionment and chemical conversions of VOCs based on a comprehensive summer observation experiment in Beijing, Atmospheric Pollution Research, 12, 230-241, https://doi.org/10.1016/j.apr.2020.12.010, 2021a.

Zhang, D., He, B., Yuan, M., Yu, S., Yin, S., and Zhang, R.: Characteristics, sources and health risks assessment of VOCs in Zhengzhou, China during haze pollution season, Journal of Environmental Sciences, 108, 44-57, https://doi.org/10.1016/j.jes.2021.01.035, 2021b.

Zhang, D., Li, X., Yuan, M., Xu, Y., Xu, Q., Su, F., Wang, S., Zhang, R.: Characteristics and sources of nonmethane volatile organic compounds (NMVOCs) and O_3–NO_x–NMVOC relationships in Zhengzhou, China, Atmosphere Chemistry and Physics, 24, 8549-8567, https://doi.org/10.5194/acp-24-8549-2024, 2024.

Zhang, F., Shang, X., Chen, H., Xie, G., Fu, Y., Wu, D., Sun, W., Liu, P., Zhang, C., Mu, Y., Zeng, L., Wan, M., Wang, Y., Xiao, H., Wang, G., and Chen, J.: Significant impact of coal combustion on VOCs emissions in winter in a North China rural site, Science of the Total Environment, 720, 137617, https://doi.org/10.1016/j.scitotenv.2020.137617, 2020.

Zhang, J., Sun, Y., Wu, F., Sun, J., and Wang, Y.: The characteristics, seasonal variation and source apportionment of VOCs at Gongga Mountain, China, Atmospheric

769 Environment, 88, 297-305, https://doi.org/10.1016/j.atmosenv.2013.03.036, 2014.

770 Zhang, Z., Yan, X., Gao, F., Thai, P., Wang, H., Chen, D., Zhou, L., Gong, D., Li,

771 Q., Morawska, L., and Wang, B.: Emission and health risk assessment of volatile

772 organic compounds in various processes of a petroleum refinery in the Pearl River Delta,

773 China, Environmental Pollution, 238, 452-461,

774 https://doi.org/10.1016/j.envpol.2018.03.054, 2018.

775 Zheng, H., Kong, S., Xing, X., Mao, Y., Hu, T., Ding, Y., Li, G., Liu, D., Li, S.,

776 and Qi, S.: Monitoring of volatile organic compounds (VOCs) from an oil and gas

777 station in northwest China for 1 year, Atmospheric Chemistry and Physics, 18, 4567-

778 4595, https://doi.org/10.5194/acp-18-4567-2018, 2018.

779 Zheng, J., Zhong, L., Wang, T., Louie, P. K. K., and Li, Z.: Ground-level ozone in

780 the Pearl River Delta region: Analysis of data from a recently established regional air

781 quality monitoring network, Atmospheric Environment, 44, 814-823,

782 https://doi.org/10.1016/j.atmosenv.2009.11.032, 2010.

783 Zhou, Z., Xiao, L., Fei, L., Yu, W., Lin M., Huang, T., Zhang, Z. and Tao J.:

784 Characteristics and sources of VOCs during ozone pollution and non-pollution periods

785 in summer in Dongguan industrial concentration area, Environmental Science, 4497-

786 4505, https://doi.org/10.13227/j.hjkx.202111285, 2022.

787 Zou, Y., Yan, X. L., Flores, R. M., Zhang, L. Y., Yang, S. P., Fan, L. Y., Deng, T.,

788 Deng, X. J., and Ye, D. Q.: Source apportionment and ozone formation mechanism of

789 VOCs considering photochemical loss in Guangzhou, China, Science of the Total

790 Environment, 903, 166191, https://doi.org/10.1016/j.scitotenv.2023.166191, 2023.

791 Zuo, H., Jiang, Y., Yuan, J., Wang, Z., Zhang, P., Guo, C., Wang, Z., Chen, Y., Wen,

792 Q., Wei, Y., Li, X.: Pollution characteristics and source differences of VOCs before and

793 after COVID-19 in Beijing, Science of The Total Environment, 907, 167694,

794 https://doi.org/10.1016/j.scitotenv.2023.167694, 2024.

795